Role of critical current on the point-contact Andreev reflection spectra between a normal metal and a superconductor

Goutam Sheet, S. Mukhopadhyay, and P. Raychaudhuri*
Department of Condensed Matter Physics and Materials Science, Tata Institute of Fundamental Research, Homi Bhabha Road, Colaba, Mumbai 400005, India
(Received 29 November 2003; revised manuscript received 2 February 2004; published 16 April 2004)

The point-contact spectrum between a normal metal and a superconductor often shows unexpected sharp dips in the conductance at voltage values larger than the superconducting energy gap. These dips are not predicted in the Blonder-Tinkham-Klapwijk (BTK) theory, commonly used to analyze these contacts. We present here a systematic study of these dips in a variety of contacts between different combinations of a superconductor and a normal metal. From the correlation between the characteristics of these dips with the contact area, we conclude that such dips are caused by the contact not being in the ballistic limit. An analysis of the possible errors introduced while analyzing such a spectrum with the standard BTK model is also presented.

DOI: 10.1103/PhysRevB.69.134507 PACS number(s): 74.50.+r, 73.23.Ad, 74.45.+c, 72.25.Ba

Andreev reflection is a process by which an electron incident from a normal metal on a normal metal/superconductor interface with energy less than the superconducting energy gap (Δ) gets converted into a Cooper pair in the superconductor, leaving a hole in the opposite spin band of the metal. Measurement of Andreev reflections using a point contact between a normal metal and a superconductor has long been used as a probe for conventional and unconventional superconductors.[1–7] In these kind of measurements, a fine tip made up of a normal metal (superconductor) is brought into mechanical contact with a superconductor (normal metal) and the differential conductance ($G=dI/dV$) versus voltage (G-V) characteristic of the microcontact is analyzed to obtain useful information regarding the superconductor, such as the value of the superconducting energy gap, symmetry of the order parameter, etc. Recently, it has been shown that this technique can also be used to obtain information on the spin polarization of a ferromagnet[8,9] by measuring the G-V characteristic of a ferromagnet/*s*-wave superconductor point contact. The point-contact Andreev reflection (PCAR) technique has been put to effective use to explore unusual superconductors such as MgB_2 and superconducting borocarbides,[3] heavy fermions,[4,5] as well as to measure the spin polarization in half-metallic ferromagnets like CrO_2 (Ref. 10) and $La_{0.7}Sr_{0.3}MnO_3$.[11]

The PCAR G-V spectrum between a normal metal and an *s*-wave superconductor is usually analyzed in the framework of the Blonder-Tinkham-Klapwijk[1] (BTK) theory, which assumes that an electron does not undergo any inelastic scattering within a spherical volume of the diameter (i.e., a) of a given point contact. This can be achieved when the contact is in the ballistic limit, i.e., when the diameter (a) of the point contact is smaller than the electronic mean free path (l) in the solid. The BTK theory predicts that, for a clean contact between a normal metal and an *s*-wave superconductor, the conductance for voltages below the superconducting gap ($V<\Delta/e$) is enhanced by a factor of 2 over that in the normal state ($V\gg\Delta/e$) due to Andreev reflection. For a real contact, a potential barrier almost always exists between the two electrodes, originating from both the oxide barrier at the interface as well as from the Fermi wave vector mismatch between the normal metal and the superconductor. This potential barrier, modeled within the BTK formalism as a δ function barrier of the form $V(x)=V_0\delta(x)$ at the interface, causes a suppression of the enhancement in $G(V)$ below the gap value, and two symmetric peaks about $V=0$ appear in the PCAR spectrum. An experimental spectrum is normally fitted with the BTK model using the strength of the potential barrier (expressed in terms of the dimensionless quantity $Z=V_0/\hbar v_F$, where v_F is the Fermi velocity in the superconductor) and Δ as fitting parameters. According to the BTK theory, for large values of this scattering barrier ($Z\rightarrow\infty$), the position of the two peaks in the conductance gives the gap value of the superconductor. For intermediate values of Z, these peaks occur at energies slightly below Δ. When a ferromagnetic metal is used as the normal metal electrode, all the Andreev reflected holes cannot propagate in the normal metal due to the difference between spin-up and spin-down densities of states at the Fermi level. This causes a suppression of the differential conductance for $V<\Delta/e$. In this case, the spectrum can be fitted with a modified BTK model,[12–14] where the transport spin polarization of the ferromagnet $[P_t=(N_\uparrow v_{F\uparrow}-N_\downarrow v_{F\downarrow})/(N_\uparrow v_{F\uparrow}+N_\downarrow v_{F\downarrow})]$ is used as a fitting parameter in addition to Z and Δ. In either case, no structure, apart from a smooth decay of the conductance to its normal state value, should appear in the spectrum above the superconducting energy gap.

In practice, the measured PCAR G-V spectrum often shows sharp dips in conductance,[2,4–8,15–19] which cannot be easily accounted for within the ambit of the BTK formalism. These dips often appear at energies larger than the superconducting energy gap and have been observed in a wide variety of combinations between normal metals and low- and high-T_c superconductors, such as Nb/Cu,[8] Nb/Pt,[19] Pt-Ir/$Bi_2Sr_2CaCu_2O_{8+\delta}$,[2] and Au-$MgB_2$,[15] as well as in combinations of normal metal tips and heavy fermion superconductors.[4,5,18] For a contact made with a conventional *s*-wave superconductor, the superconducting proximity

effect[16] in the normal metal and the intergrain Josephson tunneling[17] when the superconducting electrode is polycrystalline have been proposed as possible explanations for these dips. However, a detailed satisfactory understanding of the origin of these dips is still lacking. This hinders the extraction of reliable information on Δ or P_t from a PCAR spectrum.

In the current work, we present a systematic study of the above stated dip structures in point contacts made up of conventional superconductors and ferromagnetic and nonferromagnetic normal metals. The point contacts were made by pressing the tip on the sample using a 100 threads per inch differential screw arrangement in a liquid He cryostat in which the temperature and the magnetic field could be conveniently varied and controlled. For point contacts on superconducting samples, a mechanically cut Pt-Ir wire was used as the normal tip. For the normal samples the PCAR spectra were measured by making contacts either with electrochemically etched Nb tips or with mechanically cut Ta tips. A four-probe modulation technique operating at 362 Hz was used to directly measure the differential resistance ($R_d \sim dV/dI$) versus V characteristics, from which the differential conductance (G) was calculated, e.g., $G=1/R_d$.

In Figs. 1(a)–1(d), we show some typical point-contact spectra between Nb/Ta tips and Au, $Au_{1-x}Fe_x$, and Fe foils. Figures 1(e) and 1(f) show the spectra of a superconducting V_3Si single crystal and a polycrystalline Y_2PdGe_3 sample,[20] respectively, taken with a Pt-Ir tip. All the spectra exhibit sharp dips at voltage values above the superconducting energy gaps (as marked by arrows). The dips are qualitatively similar in all these spectra. The dips disappear close to the superconducting transition T_c or H_{c2} of the superconductor. The observation of sharp dips in Nb/Fe [see Fig. 1(c)], where Fe acts as a strong pair breaker, rules out the possibility of the superconducting proximity effect[16] playing a significant role in the origin of these dips. Also, the observation of the dips in single-crystalline V_3Si sample rules out the the possibility of intergrain Josephson tunneling[17] being a primary cause of these dips.

To investigate whether these dips are caused by the point contact not being in the pure ballistic limit, we studied the G-V spectra of a Ta/Au and an Fe/Nb point contact by successively reducing the diameter of the point contact. To obtain a series of successive spectra the superconducting tip was initially pressed on to a Au/Fe foil, giving a low-resistance, large-area contact. The tip was then gradually withdrawn in small steps so as to reduce the contact area (i.e., increasing contact resistance) without breaking the contact, and the spectra were recorded for each successive contact. Figures 2(a) and 2(b) show the spectra obtained in this way for Ta/Au and Fe/Nb point contacts, respectively. For clarity, we have plotted here R_d versus V instead of the G-V plots. Although the softness of Au allowed a better control of the point-contact diameter in the Au/Ta contact, a general trend is easily discernible in the two sets of spectra. For low-resistance, large-area contacts the two symmetric dips in the conductance (appearing as peaks in R_d) appear at voltage values larger than the corresponding superconducting energy gaps [i.e., 0.45 meV for Fig. 2(a) and 1.5 meV for Fig. 2(b)].

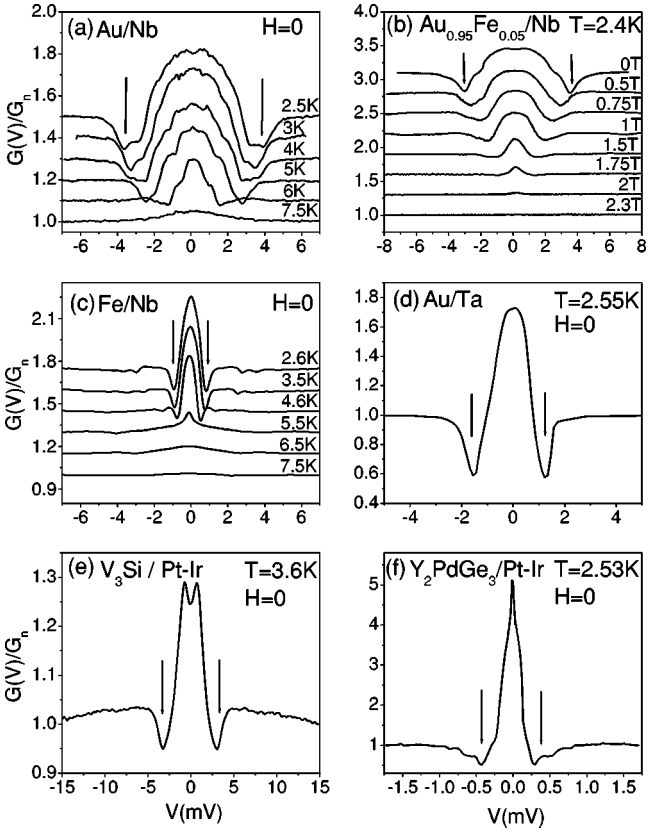

FIG. 1. Conductance versus voltage characteristics of point contacts using different superconductors and normal metals: (a) Au foil/Nb tip at different temperatures in zero field; (b) $Au_{0.95}$-$Fe_{0.05}$ foil/Nb tip in different magnetic fields at 2.43 K; (c) Fe foil/Nb tip at different temperatures in zero field; (d) Au foil/Ta tip; (e) V_3Si single crystal/Pt-Ir tip; (f) Y_2PdGe_3 polycrystalline sample/Pt-Ir tip. In (f) a zero-bias enhancement of the order of 5 is observed. Sharp dips in conductance are observed for all spectra (marked by arrows) at voltage values larger than the corresponding superconducting energy gaps. All curves shown in (a)–(c) except the bottom curve in each case are shifted upward for clarity.

As the point-contact diameter is reduced, these dips gradually disappear, and the spectra tend toward the spectra predicted by BTK theory.[21]

To comprehend the gradual emergence of the dips with increasing point-contact diameter, we note that a point contact between the two metals can be categorized into three broad regimes[18,22] depending on the size a. In the ballistic regime, where $l \gg a$, an electron can accelerate freely within a length a from the point contact, with no heat generated in the contact region. For two normal metals (or a metal and a superconductor at voltages $V \gg \Delta/e$) the contact resistance in this limit is given by the Sharvin resistance $R_s = 2(h/e^2)/(ak_F)^2$. In the opposite scenario, when $l \ll a$, the potential varies smoothly over a radius a of the point contact due to the inelastic scattering. In this case, power gets dissipated in the contact region, thereby increasing the effective temperature of the point contact. The contact resistance in such a circumstance is governed by the Maxwell resistance $R_M = \rho(T_{\text{eff}})/2a$, where $\rho(T)$ is the bulk resistivity and T_{eff} is the effective temperature of the point contact. The heat dis-

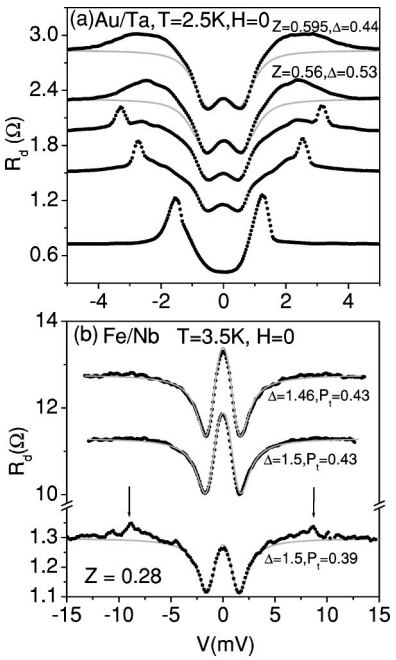

FIG. 2. Evolution of PCAR spectra for (a) Au/Ta (b) Fe/Nb point contact with normal state contact resistance $R_d(V \gg \Delta/e)$ of the contact (solid circles). Solid lines in the two topmost curves in panels (a) and (b) are BTK fits with fitting parameters as shown in the figure. The appearance of two peaks at voltage values higher than Δ/e for $R_d(V \gg \Delta/e) = 1.3\,\Omega$ in (b) is shown with arrows. Some curves have been omitted for clarity.

sipated in the point contact in this regime is primarily carried by the conduction electrons. When the Wideman-Franz law holds it can be shown that the effective temperature is related to the applied voltage through the relation $T_{\text{eff}}^2 = T^2 + V^2/4L$, where L is the Lorentz number.[23] When the situation does not conform to one of these two extreme regimes, the contact resistance is given by $R = R_s + \Gamma(l/a)R_M$ where $\Gamma(l/a)$ is a slowly varying function of the order of unity. Since $R_s \sim (1/a)^2$ whereas $R_M \sim (1/a)$, the Sharvin contribution to the resistance will increase more rapidly than the Maxwell contribution with decreasing contact area, and for very small area it will go toward the pure ballistic limit. In between these two regimes there also exists a diffusive regime, for which the contact diameter is smaller than the inelastic scattering length, but is larger than the elastic mean free path. In this case, no significant heating occurs at the contact, but the Andreev reflection is suppressed as compared to that in the ballistic case.[12,13] A point of caution here is that the relationship for R_M strictly holds only for contacts between similar metals. For dissimilar metals, an effective $\rho(T)$ ought to be substituted, which could be a weighted average of the $\rho(T)$ of the two metals.

Within the above scenario, it is now possible to account for the gradual surfacing of the dips with the increase in the resistance value of the point contact. In the data of superconductor–normal metal contacts as shown in Figs. 2(a) and 2(b) the tip is initially pressed on the sample to generate a low-resistance–large-area contact. These contacts are expected to be in the thermal regime, where the point-contact resistance is determined by the bulk resistivity of the two electrodes. At low current values through the point contact, the resistivity of the superconductor is zero. The contact resistance will therefore have a contribution from R_s and a small contribution from R_M coming from the finite resistivity of the normal electrode. However, as the transmitted current through the point contact reaches the limiting critical current value (I_c) of the superconductor, the resistivity of the superconductor rapidly increases to its normal state value. Therefore, as the current reaches I_c, one would expect a sharp rise in the voltage across the junction, and consequently a dip in the differential conductance ($G = dI/dV$). As the differential screw making the point contact is gradually withdrawn, the contribution of R_M to the point-contact resistance decreases and the contribution of the Andreev current increases. Since the R_M/R_s ratio decreases with decreasing a the dips become smaller and the spectrum takes the shape in conformity with BTK theory. To illustrate this point further, we have simulated the differential resistance versus voltage characteristics of the point contact, assuming that above the critical current of the superconducting tip, the voltage across the point contact consists of both the Sharvin contribution (V_s) of the normal-normal contact and the Maxwell contribution (V_M) arising from the finite resistivity of the superconductor. V_s is calculated from the BTK model [solid line in Fig. 3(a)]. For $V \gg \Delta/e$, where Andreev reflection is suppressed, this gives the voltage contribution arising from the Sharvin resistance of the normal-normal contact.[1] For the superconductor above the critical current, a typical I-V curve such as the one shown with a dashed line in Fig. 3(a) is assumed. At high bias where the superconductor is in the normal state, this voltage (V_M) is proportional to R_M of the normal-normal contact. Since for a given current the voltage drop across the point contact is given by $V = V_M + V_s$, the I-V characteristic of a contact with a particular R_M/R_s ratio is simulated by scaling the dashed curve with respect to the solid curve such that at the highest bias current $V_M/V_s = R_M/R_s$.[24] The differential resistance versus voltage for different values of R_M/R_s at $V \gg \Delta/e$ calculated by differentiating the I-V curves generated in this way is shown with open circles in Fig. 3(a). Although the assumed I-V curve of the superconductor is empirical, the trends in Fig. 3(a) conforms to the experimental data: With increasing contribution from R_M (i) two pronounced peaks appear in R_d at $V > \Delta/e$ [marked by arrows in Fig. 3(a)] and (ii) there is an increase in the relative enhancement in the zero-bias conductance compared to its high-bias value. It is interesting to note that if a contact is made between a good normal metal and a superconductor with very large normal state resistivity (where the contact is likely to be in the thermal regime due to the short mean free path in the superconductor and because $R_M/R_s > 1$), a several-fold enhancement in the $G(V=0)$ value compared to $G(V \gg \Delta/e)$ is expected, arising from the critical current alone. Such a behavior is evident in Fig. 1(f), where a five-fold enhancement is present in a contact made between an Y_2PdGe_3 polycrystalline sample (with normal state resistivity $\sim 400\ \mu\Omega\,\text{cm}$) and a Pt-Ir tip. A similar explanation such as the one outlined here for the occurrence of dips in the PCAR spectra in amorphous $(Mo_{0.55}Ru_{0.45})_{0.8}P_{0.2}$ was pro-

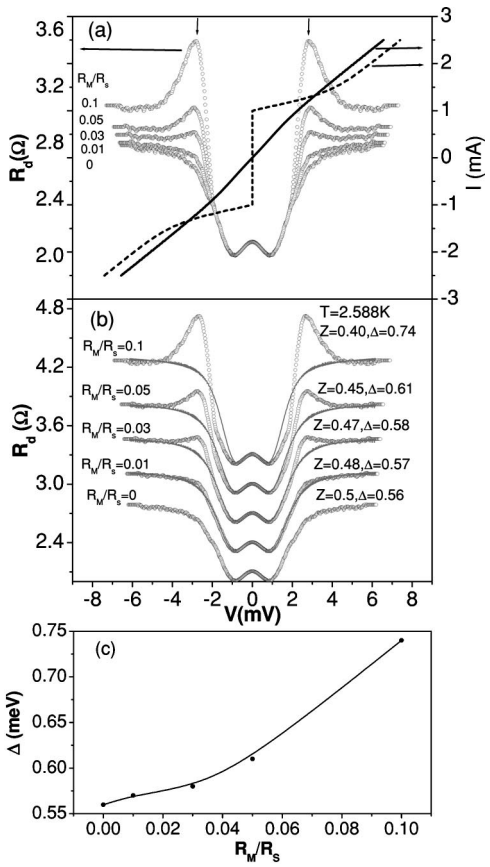

FIG. 3. Current versus voltage characteristics of a superconductor/normal metal point contact generated theoretically, adding the effect of critical current over the BTK model. (a) The solid and dashed lines are the I-V characteristics obtained from the BTK model (with $Z=0.5$ and $\Delta=0.56$ meV) and the typical I-V characteristic assumed for the superconductor, respectively. R_d vs V curves (open circles) for different R_M to R_s ratios are shown in the same figure. Two sharp peaks symmetric about $V=0$ (shown by arrows) in the R_d vs V spectra arise and become sharper with increasing R_M/R_s. (b) BTK fits of the curves generated in (a) neglecting the contribution of the critical current. Solid lines show the fits and open circles are generated R_d versus V with different R_M/R_s ratios. A vertical shift has been given to all curves except the bottom one for clarity. (c) Variation of Δ obtained by fitting the curves generated in (a) with the BTK model.

posed by Häussler *et al.*[25] However, their explanation was based on the formation of a single vortex in the type II superconductor when the current reaches a critical value. We have shown that the origin of the dips is more general; namely, they occur for both type I (Ta) and type II (Nb) superconductor when the current reaches I_c, and not necessarily associated with the formation of a vortex at the point contact.

In the above context it becomes pertinent to carefully examine the analysis of the point-contact spectra in the presence of dips in the conductance. It is apparent from Fig. 2(a) that, even for the smallest-diameter Au/Ta contact that we could stabilize, the conductance has a finite contribution from R_M. The G-V curve calculated from the BTK model is indeterminate within a proportionality constant, which depends on the contact diameter as well as on the densities of states and Fermi velocities in the two metals. A general practice when analyzing a point-contact spectrum comprised of dips is to fit it with the BTK model while ignoring these dips, using Δ and Z as the fitting parameters, and determine the proportionality factor by normalizing the calculated G-V curve to the experimental value of conductance at a high bias value. The result of such fits for the two uppermost Ta/Au point-contact spectra in Fig. 2(a) is shown with solid lines. This analysis ignores the fact that at high bias the measured $R_d(V \gg \Delta/e)$ values for these spectra contain contributions from both R_s and R_M whereas the spectra calculated from the BTK model will have a contribution only from R_s. A quantitative estimate of the contribution from R_M is difficult without a detailed knowledge of the I-V characteristic of the superconductor above the critical current. To get a qualitative understanding of the error involved in this kind of fits, we tried to fit the calculated curves in Fig. 3(a) (generated by adding a finite contribution from R_M) with BTK model alone, ignoring the contribution of the finite resistivity of the superconductor above I_c [see Fig. 3(b)]. Although with suitable choice of Z and Δ the curves can be fitted for bias voltages below and above the dips, the values of Δ are overestimated. Figure 3(c) shows how this error increases with increasing R_M/R_s ratio in the spectrum. Although this procedure may introduce a small error when the dips are small, it will introduce a significant error in Δ when the dips are large. Similarly, for a contact between a ferromagnet and a superconductor P_t is underestimated as the contribution from R_M increases. This trend can be seen in the fits shown in Fig. 2(b).

As a consistency check of the proposed explanation of the dips, we can also try to estimate the critical current density (J_c) of the superconductor from the observed dips. When the contribution of R_M in the spectra is small the normal state differential resistance is $R_d(V \gg \Delta/e) \approx R_s = 2(h/e^2)/(ak_F)^2$. For Au,[26] $k_F \sim 1.21 \times 10^8$ cm^{-1}. This gives the contact diameter $a \sim 120$ Å for the Au-Ta contact with $R_d(V \gg \Delta/e) = 2.8\,\Omega$. A rough estimate of the critical current can be obtained from the voltage at which the experimental curve deviates from the BTK best fit. Comparing this voltage with the corresponding current in the I-V curve, obtained by integrating the G-V curve, we get a critical current of 0.41 mA. This gives $J_c \sim 3.6 \times 10^8$ A/cm^2 a reasonable number considering the approximations involved.

It should be noted that in the preceding analysis we have neglected the effect of contact heating on the critical current of the superconductor. Since contact heating primarily happens due to the contribution from Maxwell resistance, this assumption is justified for low area contacts where R_M/R_s is small. However, for very large-area, low-resistance contacts (where $R_M/R_s \gg 1$), significant heat dissipation will occur at the contacts. For these contacts the effective temperature (T_{eff}) of the contact will rise rapidly with applied voltage. Using the expression $T_{\text{eff}}^2 = T^2 + V^2/4L$ and substituting the value for the Lorenz number, we get a rise in T_{eff} at the rate[23] of 3.2 K/mV at $T=0$. At low temperatures the contact heating will therefore drive the superconductor into the normal

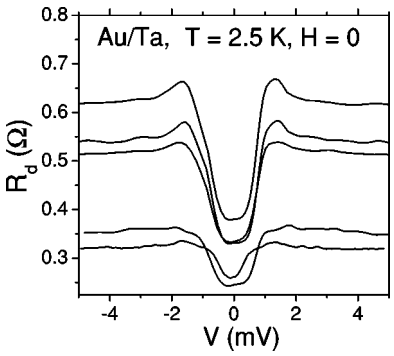

FIG. 4. R_d versus V for Au-Ta point contacts with very low normal state resistance $R_d(V \gg \Delta/e)$. In this regime the shape of the spectrum is dominated by heating at the point contact.

state before the current reaches the critical value. In this case no sharp dip will be observed in the spectrum, but the G-V characteristics will not show any feature associated with Andreev reflection. A few examples of this kind of Au-Ta contact with very low resistance are shown in Fig. 4. The dips in the conductance gradually start appearing in this regime as the point-contact diameter is reduced, thereby driving the contact away from the thermal regime.

In principle, one could also think of an opposite situation where the contact is in the ballistic limit but where the superconductor reaches I_c at voltage values smaller than or of the order of Δ/e. Since the features unambiguously associated with Andreev reflection occur in the voltage range $\pm 2\Delta/e$, one would get a spectrum with sharp dips and no feature associated with Andreev reflection will appear. Of the many contacts studied, we never observed any spectra of this kind. This possibility should, however, be kept in mind while studying superconductors with very low critical current densities or at temperatures close to T_c where the critical current is small.

In summary, we have presented a study of the emergence of anomalous dips in the conductance in point contacts between normal metals and conventional superconductors. From the correlation between the structure of the dips and the area of contact, we conclude that the dips arise from the finite resistivity of the superconducting electrode above the critical current when the contact is not in the ballistic limit. We have also shown that in the thermal limit of the point contact an enhancement of the zero bias conductance larger than twice the value at high bias can be observed if the contact is made between a good normal metal and a superconductor with large normal state resistivity. It is useful to recall that in unconventional superconductors this kind of enhancement has been observed and often attributed to the formation of Andreev bound states. It could be worthwhile to explore the extent to which R_M may contribute in the enhancement of zero-bias conductance even in such systems.

We would like to acknowledge Professor A. K. Nigam and Professor E. V. Sampathkumaran for providing samples of $Au_{1-x}Fe_x$ and Y_2PdGe_3, respectively, and Professor S. Ramakrishnan and Professor H. Küpfer for single crystals of V_3Si. We would like to thank Professor S. Bhattacharya for encourangement and guidance and Professor A. K. Grover for critically reading the manuscript. Two of us (G.S. and S.M.) would like to acknowledge the TIFR Endowment Fund for partial financial support.

*Electronic mail: pratap@tifr.res.in

[1] G. E. Blonder, M. Tinkham, and T. M. Klapwijk, Phys. Rev. B **25**, 4515 (1982).

[2] Y. DeWilde *et al.*, Phys. Rev. Lett. **80**, 153 (1998).

[3] P. Szabo, P. Samuely, J. Kacmarcik, T. Klein, J. Marcus, D. Fruchart, S. Miraglia, C. Marcenat, and A. G. M. Jansen, Phys. Rev. Lett. **87**, 137005 (2001); I. K. Yanson, N. L. Bobrov, C. V. Tomy, and D. McK. Paul, Physica C **334**, 33 (2000).

[4] Ch. Walti, H. R. Ott, Z. Fisk, and J. L. Smith, Phys. Rev. Lett. **84**, 5616 (2000).

[5] Y. DeWilde, J. Heil, A. G. M. Jansen, P. Wyder, R. Deltour, W. Assmus, A. Menovsky, W. Sun, and L. Taillefer, Phys. Rev. Lett. **72**, 2278 (1994).

[6] Z. Q. Mao, M. M. Rosario, K. D. Nelson, K. Wu, I. G. Deac, P. Schiffer, Y. Liu, T. He, K. A. Regan, and R. J. Cava, Phys. Rev. B **67**, 094502 (2003).

[7] F. Laube, G. Goll, H. v. Lohneysen, M. Fogelstrom, and F. Lichtenberg, Phys. Rev. Lett. **84**, 1595 (2000).

[8] R. J. Soulen, Jr. *et al.*, Science **282**, 85 (1998).

[9] S. K. Upadhyay, A. Palanisami, R. N. Louie, and R. A. Buhrman, Phys. Rev. Lett. **81**, 3247 (1998).

[10] Y. Ji, G. J. Strijkers, F. Y. Yang, C. L. Chien, J. M. Byers, A. Anguelouch, Gang Xiao, and A. Gupta, Phys. Rev. Lett. **86**, 5585 (2001).

[11] B. Nadgorny, I. I. Mazin, M. Osofsky, R. J. Soulen, P. Broussard, R. M. Stroud, D. J. Singh, V. G. Harris, A. Arsenov, and Y. Mukovskii, Phys. Rev. B **63**, 184433 (2001).

[12] I. I. Mazin, A. A. Golubov, and B. Nadgorny, J. Appl. Phys. **89**, 7576 (2001).

[13] N. Auth, G. Jacob, T. Block, and C. Felser, Phys. Rev. B **68**, 024403 (2003).

[14] P. Raychaudhuri, A. P. Mackenzie, J. W. Reiner, and M. R. Beasley, Phys. Rev. B **67**, 020411 (2003).

[15] Zhuang-Zhi Li, Hong-Jie Tao, Yi Xuan, Zhi-An Ren, Guang-Can Che, and Bai-Ru Zhao, Phys. Rev. B **66**, 064513 (2002).

[16] G. J. Strijkers, Y. Ji, F. Y. Yang, C. L. Chien, and J. M. Byers, Phys. Rev. B **63**, 104510 (2001).

[17] L. Shan, H. J. Tao, H. Gao, Z. Z. Li, Z. A. Ren, G. C. Che, and H. H. Wen, Phys. Rev. B **68**, 144510 (2003).

[18] K. Gloos *et al.*, J. Low Temp. Phys. **105**, 37 (1996); see also Phys. Rev. Lett. **85**, 5257 (2000).

[19] H. Srikanth and A. K. Raychaudhuri, Phys. Rev. B **46**, 14 713 (1992).

[20] Subham Majumdar and E. V. Sampathkumaran, Phys. Rev. B **63**, 172407 (2001).

[21] The systematic evolution from the ballistic to the thermal regime with decreasing $R_d(V \gg \Delta/e)$ is not always observed when the tip is reengaged on the sample. The primary reason for this is that in addition to the contact area the point-contact resistance is also determined by Z, which depends on the oxide barrier at the

interface. The nature of this barrier varies from contact to contact when the tip is reengaged.

[22] For a review of point-contact spectroscopy, see A. M. Duif, A. G. M. Jansen, and P. Wyder, J. Phys.: Condens. Matter **1**, 3157 (1989).

[23] For a detailed discussion of point-contact heating, see Yu. G. Naidyuk and I. K. Yanson, "*Point Contact Spectroscopy*" [physics/0312016 (unpublished)].

[24] Strictly speaking, this analysis should take into account the fact that the I-V curve will have no contribution from Andreev reflection after the current reaches the critical current. However, for all the spectra discussed here, the dips in the conductance are observed at voltage values larger than $\pm 2\Delta/e$. At these voltages Andreev reflection is already suppressed, and taking this effect explicitly into account changes the shape of the spectrum only slightly.

[25] R. Häussler, G. Goll, Yu. G. Naidyuk, and H. v. Löhneysen, Physica B **218**, 197 (1996).

[26] N. W. Ashcroft and D. Mermin, *Solid State Physics* (Harcourt, Singapore, 1976).